Ozone-derived Oxysterols Affect Liver X Receptor (LXR) Signaling
A POTENTIAL ROLE FOR LIPID-PROTEIN ADDUCTS*

Adam M. Speen[‡], Hye-Young H. Kim[§], Rebecca N. Bauer[‡], Megan Meyer[‡], Kymberly M. Gowdy[¶], Michael B. Fessler[∥], Kelly E. Duncan[‡], Wei Liu[§], Ned A. Porter[§], and Ilona Jaspers[‡1]

From the [‡]Curriculum in Toxicology, Departments of Pediatrics and Microbiology and Immunology, Center for Environmental Medicine, Asthma, and Lung Biology, University of North Carolina, Chapel Hill, North Carolina 27599, the [§]Department of Chemistry and Center for Molecular Toxicology, Vanderbilt University, Nashville, Tennessee 37235, the [¶]Department of Pharmacology and Toxicology, Brody School of Medicine, East Carolina University, Greenville, North Carolina 27834, and the [∥]Immunity, Inflammation, and Disease Laboratory, NIEHS, National Institutes of Health, Research Triangle Park, North Carolina 27709

Edited by Dennis Voelker

When inhaled, ozone (O_3) interacts with cholesterols of airway epithelial cell membranes or the lung-lining fluid, generating chemically reactive oxysterols. The mechanism by which O_3-derived oxysterols affect molecular function is unknown. Our data show that *in vitro* exposure of human bronchial epithelial cells to O_3 results in the formation of oxysterols, epoxycholesterol-α and -β and secosterol A and B (Seco A and Seco B), in cell lysates and apical washes. Similarly, bronchoalveolar lavage fluid obtained from human volunteers exposed to O_3 contained elevated levels of these oxysterol species. As expected, O_3-derived oxysterols have a pro-inflammatory effect and increase NF-κB activity. Interestingly, expression of the cholesterol efflux pump ATP-binding cassette transporter 1 (ABCA1), which is regulated by activation of the liver X receptor (LXR), was suppressed in epithelial cells exposed to O_3. Additionally, exposure of LXR knock-out mice to O_3 enhanced pro-inflammatory cytokine production in the lung, suggesting LXR inhibits O_3-induced inflammation. Using alkynyl surrogates of O_3-derived oxysterols, our data demonstrate adduction of LXR with Seco A. Similarly, supplementation of epithelial cells with alkynyl-tagged cholesterol followed by O_3 exposure causes observable lipid-LXR adduct formation. Experiments using Seco A and the LXR agonist T0901317 (T09) showed reduced expression of *ABCA1* as compared with stimulation with T0901317 alone, indicating that Seco A-LXR protein adduct formation inhibits LXR activation by traditional agonists. Overall, these data demonstrate that O_3-derived oxysterols have pro-inflammatory functions and form lipid-protein adducts with LXR, thus leading to suppressed cholesterol regulatory gene expression and providing a biochemical mechanism mediating O_3-derived formation of oxidized lipids in the airways and subsequent adverse health effects.

Currently, the oxidant gas ozone (O_3) is the most widespread air pollutant found in the United States and contributes to a growing variety of adverse health outcomes (1). O_3 exposure causes decreased lung function and increased airway inflammation, which exacerbates pre-existing diseases such as asthma and may contribute to certain cardiovascular diseases, all potentially increasing the risk of premature death (2). Although the inflammatory response and adverse health effects of O_3 exposure have been documented for decades, the biochemical and cellular mechanisms by which O_3 mediates adverse health effects remain poorly understood. As a very potent oxidant gas, O_3 reacts readily with the surface components of the airway and causes cellular modification through reactions with the airway-lining fluid and epithelial cellular membranes (2–4). The lung-lining fluid and epithelial cell membranes are rich in cholesterol and other lipids, which can be directly oxidized by O_3 (5, 6). Previous studies have determined the impact that ozonization of lipids, particularly polyunsaturated fatty acids (PUFA), may have on O_3-associated toxic effects. These studies demonstrated that ozonization of PUFAs and the formation of lipid ozonization products can mimic many of the adverse health effects observed after exposure to O_3 (5, 7–9). However, the involvement of cholesterol ozonization products requires further study. The cholesterol 5,6-double bond and concomitant vinylic methylene group moieties are particularly susceptible to oxidation, resulting in the formation of oxysterols (5, 10–12).

Many oxysterols are electrophiles capable of reacting with nucleophilic residues on proteins and other biological macromolecules. They are formed endogenously through enzy-
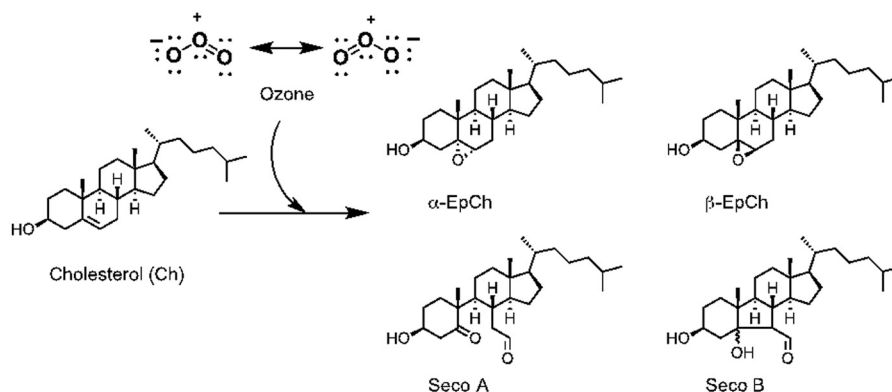
FIGURE 1. **Cholesterol and the major oxysterols formed in the reaction with ozone.**

matic and non-enzymatic reactions. P450 cytochrome enzymes metabolize endogenous cholesterol into oxysterol species such as 27-hydroxycholesterol, an essential oxysterol for cellular cholesterol homeostasis (13). Studies show that endogenous oxysterols can act as both agonists and antagonists for transcription factors such as the liver X receptor (LXR).[2] Within the LXR protein, a ligand binding domain has been characterized and shown to bind to synthesized oxysterol species *in vitro*, which is the same region that is the target for various post-translational modifications such as acetylation and SUMOylation (14). LXR regulates the synthesis of cholesterol transport proteins, such as ATP-binding cassette transporter A1 (ABCA1). ABCA1 transports cholesterol across the cell membrane and shuttles it onto apolipoproteins, resulting in the formation of high density lipoproteins (HDL). Systemically, failure to produce adequate ABCA1 reduces the ability to generate and transport HDL and is associated with early onset cardiovascular disease, supporting the protective role of ABCA1 in cholesterol metabolism and atherosclerosis (15). In addition to lipid metabolism, both LXR and ABCA1 have been implicated in anti-inflammatory functions (16–19). Moreover, exogenously derived oxysterols can cause adverse cellular effects and have been shown to modulate host immune cell and inflammatory responses (20–22). Oxidation of endogenous cholesterols by various reactive oxygen species results in the formation of oxysterols associated with various pathological processes driven by interaction with the nucleophilic domains of key proteins (23). Elevated levels of specific oxysterol species have been linked to a variety of adverse biological activities, including cytotoxicity, increased inflammation, and amplified infection (24–26).

Rodent exposure studies and *in vitro* studies using human pulmonary surfactant have demonstrated the formation of O_3-derived oxidized cholesterol products in various chemical compositions (5, 6, 10, 27, 28). Fig. 1 depicts the primary reactive O_3-derived oxysterol products secosterol A (Seco A) along with its aldol condensation product secosterol B (Seco B), and epoxycholesterols α and β (α-EpCh and β-EpCh) (11, 29). Some of these O_3-derived oxysterols have been found in atherosclerotic tissue and cause foam cell formation, a hallmark of plaque buildup (26). Despite increased interest in the role of oxysterols in human health, especially cardiovascular diseases, information about O_3-derived oxysterols in the airway, their cellular targets, and their biochemical interactions is very limited.

We hypothesize that exposure to O_3 generates lipid-derived electrophiles in the human airway, including reactive species of oxysterols, at or near the epithelial surface that can adduct to cellular proteins, thus ultimately affecting cellular function and inflammatory response. Our study is designed to uncover electrophilic interactions between O_3-derived oxysterols and proteins as a new mechanistic paradigm mediating adverse health effects induced upon inhalation of O_3.

Results

Identification of O_3-induced Oxysterol Formation in Vitro and in Vivo—Primary differentiated HBEC cells and 16HBE cells were chosen to evaluate the presence of oxysterol species *in vitro* following exposure to O_3. Representative HPLC-MS profiles reflected increased levels of oxysterol species in O_3-exposed 16HBE cells (Fig. 2*A*) compared with filtered air-exposed cells. 16HBE cells exposed to O_3 exhibited elevated concentrations of α-EpCh, β-EpCh, and Seco B in cell lysates (Fig. 2*B*) and in the apical washes (Fig. 2*C*) collected both 1 and 24 h post-exposure compared with the air-exposed control. A similar trend was observed in primary HBEC lysates (Fig. 2*D*) and apical washes (Fig. 2*E*) at both 1 and 24 h post-exposure compared with air-exposed controls. Overall, the cholesterol concentration did not significantly change due to O_3 exposure or sample collection time in either 16HBE (4870 ± 597 ng/sample air to 5168 ± 138 ng/sample O_3) or primary HBE (50121 ± 1554 ng/sample air to 5506 ± 772 ng/sample O_3) cells.

To test the formation of O_3-derived oxysterols in humans *in vivo*, we determined the levels of oxysterols identified in BALF obtained from healthy volunteers exposed to filtered air or 0.3 ppm O_3 for 2 h. The BALF was collected by bronchoscopy at 1 and 24 h post-exposure, and various oxysterol species were

⧨SASBMB

FIGURE 2. **Oxysterol concentrations measured in cells and apical washes exposed to filtered air or O$_3$ and their HPLC-MS profiles.** All cells were grown in 24-mm Transwell membrane plate until confluency followed by removal of the apical medium and exposure to filtered air or 0.4 ppm O$_3$ for 4 h. Cell lysates and apical washes were collected at 1 and 24 h post-exposure. *A,* representative reverse phase-HPLC-multiple reaction monitoring chromatograms of epithelial cells exposed to air or 0.4 ppm ozone. MS for each panel is selected reaction monitoring of the *m/z* indicated in the air exposure. *B,* 16HBE cell lysate. *C,* 16HBE apical wash. *D,* primary HBEC cell lysate. *E,* primary HBEC apical wash. Data are presented as means ± S.E. Statistical analysis was performed with a one-way ANOVA and Fisher's LSD post hoc test comparing observed means against the respective air-exposed control. *, $p < 0.05$. $n = 3$.

quantified by HPLC-MS. Exposure to O$_3$ significantly elevated the concentrations of β-EpCh (Fig. 3*B*) and Seco A (Fig. 3*C*) compared with individuals exposed to filtered air controls at 1 h

post-exposure with *p* values of less than 0.001 and 0.05 respectively. A moderately convincing increase ($p < 0.1$) was observed for α-EpCh (Fig. 3*A*) and no difference in Seco B (Fig. 3*D*).

FIGURE 3. **Oxysterol concentrations measured in airway BALF.** Healthy individuals were exposed to either filtered air (control) or 0.3 ppm O_3 for 2 h. Cell-free BALF was collected by bronchoscopy at 1 and 24 h post-exposure. Oxysterols were quantified by HPLC-MS spectrometry. *A,* α-EpCh. *B,* β-EpCh. *C,* Seco A. *D,* Seco B. Data are presented as means $\pm$ S.E. Statistical analysis was performed with paired Student's *t* test (two-tailed distribution, pairing based on subject). *, $p < 0.05$; **, $p < 0.001$. $n = 9$–11.

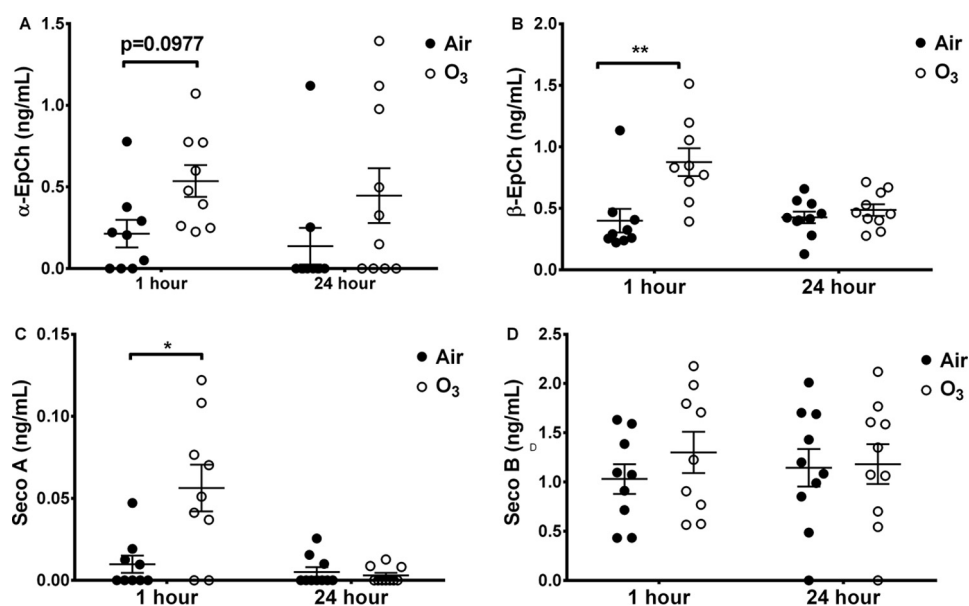Unlike the results observed in the *in vitro* samples, we observed that oxysterol concentrations returned to baseline levels 24 h post-exposure. Again, there was no significant change in overall BALF cholesterol concentration in subjects exposed to air (6639 $\pm$ 1556 ng/ml) compared with O_3 (6698 $\pm$ 2245 ng/ml).

Effects of O_3 on Cholesterol Efflux and Cytokine Gene Expression—As expected and previously described by us (30, 31), exposure to O_3 caused an inflammatory response as marked by increased gene expression (Fig. 4, *A* and *B*) and protein concentration (Fig. 4, *C* and *D*) of pro-inflammatory cytokines IL6 and IL8. Treatment with synthetic LXR agonist T0901317 (T09) alone did not affect the levels of *IL6* or *IL8* expression (Fig. 4, *A* and *B*). Interestingly, exposure to O_3 in the presence of T09 significantly decreased the expression of cholesterol efflux pump proteins *ABCG1* (Fig. 4*E*) and *ABCA1* (Fig. 4*F*), suggesting O_3-induced inhibition of the LXR pathway. Additionally, ABCA1 protein levels were significantly reduced in cells exposed to O_3 compared with air as shown in relative densitometry from three separate experiments (Fig. 4*G*) and representative immunoblot (Fig. 4*H*).

LXR-$\alpha^{-/-}$ Mice Are More Susceptible to O_3-induced Inflammation—Female LXR$\alpha^{-/-}$ were compared with WT mice. Each were exposed to filtered air or 2 ppm O_3 for 3 h. BALF was collected from both conditions and evaluated for concentrations of IL6. The LXR-$\alpha^{-/-}$ mice showed significantly higher concentrations of IL6 compared with the WT (Fig. 5*A*). At necropsy, the lungs were removed and homogenized for RNA isolation and qPCR analysis. In a similar result, IL6 mRNA levels were significantly higher in the LXR-$\alpha^{-/-}$ mice exposed to O_3 compared with the WT control mice exposed to O_3 (Fig. 5*B*). As seen in the human BALF samples (Fig. 3, *C* and *D*), exposure to O_3 increases the amount of Seco A (Fig. 5*C*) and Seco B (Fig. 5*D*) in the mouse BALF samples with significantly higher amounts of Seco A present in the LXR-$\alpha^{-/-}$ compared with the WT mice. Interestingly, unlike the human

samples, total cholesterol levels decreases in O_3-exposed animals (Fig. 5*E*).

Exposure to a-Seco A Reveals LXR-α Protein Adducts—Based on recent studies demonstrating oxysterol-induced lipid-protein adducts, we hypothesized that O_3-derived oxysterols can adduct to the LXR-α and LXR-β proteins, which contain reactive lysine residues (14, 29). Seco A, a primary ozonide and one of the most reactive O_3-derived oxysterols, reacts with proteins and causes covalent modifications leading to lipid-protein adduct formation (32). 16HBE cells were treated with alkynyl-tagged Seco A (*a*-Seco A), and the adducted proteins were identified by first adding biotin to the alkynyl tag utilizing click cyclo-addition (Fig. 6*A*) followed by immunoaffinity purification with streptavidin beads and photo-release (Fig. 6*B*), which frees cellular proteins adducted by *a*-Seco A. This mixture of proteins was subsequently subjected to Western blotting analyses using antibodies against HSP90, LXR-α, LXR-β, PPAR-γ, and β-actin (Fig. 6*C*). HSP90 was used as a positive control based on previous studies (33). Our data show that treatment of bronchial epithelial cells with *a*-Seco A results in the formation of Seco A-LXR adducts.

Alkynyl Cholesterol-supplemented Cells Exposed to O_3 Reveal the Formation of LXR-α Adducts—16HBE cells were supplemented with 20 μM alkynyl-tagged cholesterol (*a*-Chol) for 6 days. Media containing *a*-Chol changed daily with washes on the apical side 24 h prior to exposure (Fig. 7*B*). The 16HBE cells were exposed to filtered air or 0.4 ppm O_3 for 4 h and harvested 1 h post-exposure. Our data show that *a*-Chol, a surrogate of endogenous cholesterol, is incorporated into the cells and, in response to O_3, generates a host of alkynyl-oxysterols identical to the oxysterol species generated via oxidation of endogenous cholesterol (Fig. 7*A*). Based on streptavidin analysis, cells exposed to O_3 exhibit a higher overall level of protein adduction with oxidized cholesterol species than cells exposed to air (Fig. 7*C*). Similar to cells treated with *a*-Seco A, HSP90 and LXR-α
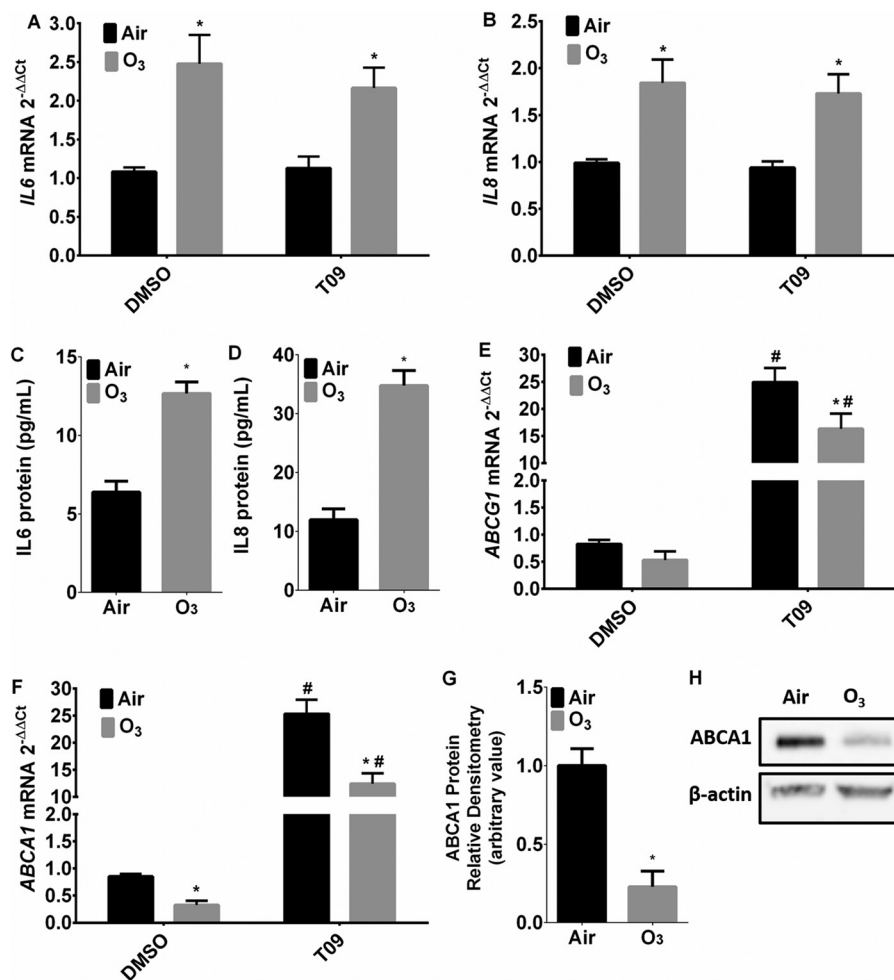
FIGURE 4. **Cholesterol efflux pump protein and pro-inflammatory cytokine gene expression levels in 16HBE cells.** Cells were exposed to filtered air or 0.4 ppm ozone for 4 h with and without 10 μM T09. RNA and apical wash samples were collected 1 h post-exposure and analyzed. Inflammatory gene expression levels *IL6* (*A*), *IL8* (*B*), and protein levels IL6 (*C*) and IL8 (*D*) as well as gene expression levels for *ABCG1* (*E*) and *ABCA1* (*F*) were measured. Additionally, ABCA1 protein levels were evaluated by immunoblot (*G*) and relative densitometry (*H*) from three separate experiments. Data are presented as means $\pm$ S.E. Statistical analysis was performed with a one-way ANOVA and Fisher's LSD post hoc test comparing observed means against the respective treatment/air-exposed control, *, $p < 0.05$, or against the DMSO/air-exposed vehicle control, #, $p < 0.05$, $n = 3$.

were found to be targets of alkynyl-tagged oxysterols generated endogenously in cells exposed to O_3 (Fig. 7D). The broad band of LXR antibody-reactive proteins shown in Fig. 7D (*Elute+O_3*) suggests that a set of O_3-derived adducts are formed under conditions of endogenous oxysterol genesis. This is in contrast to the homogeneous protein adduct observed after exposure to a single exogenous electrophile, as shown in Fig. 6C for the experiment with *a*-Seco A. Fig. 7E shows the densitometric analysis of O_3-derived adducts of LXR-α from three separate experiments.

Oxysterol Exposure Alters ABCA1, FASN, and SREBP1 Gene Transcription—Considering the effects of oxysterols on adduct formation with LXR, we evaluated whether exposure to oxysterols can alter expression levels of genes controlling cholesterol biosynthesis, fatty acid synthesis, and cholesterol efflux in 16HBE cells. To determine whether oxysterol adduct formation with LXR inhibits subsequent activation of LXR, we sequentially treated 16HBE cells with DMSO, Seco A, or T09 for 2 h, removed the first treatment, and followed with a second challenge for 2 h (Fig. 8A). Treatment with Seco A followed by T09 significantly suppressed *ABCA1* (Fig. 8B), *FASN* (Fig. 8C), and

SREBP1 (Fig. 8D) gene expression compared with cells exposed to DMSO followed by T09 and T09 followed by T09, suggesting that initial treatment with Seco A reduces the ability of T09 to enhance cholesterol synthesis and efflux gene expression. Challenge with individual oxysterol species yielded no significant change in LXRE activity when compared with the DMSO vehicle control (Fig. 8E). However, LXRE activity was significantly reduced in cells sequentially treated with Seco A followed by T09 compared with cells sequentially treated with DMSO followed by T09 or T09 followed by T09 (Fig. 8F), again suggesting that initial treatment with Seco A reduces the ability of T09 to activate LXR.

Exposure to Individual Oxysterols Activates the Inflammatory Gene Transcription Pathway—To determine whether O_3-derived oxysterols modify expression of inflammatory genes alone and in relation to known agonists, 16HBE cells were sequentially treated with DMSO, Seco A, or T09 for 2 h followed by a second challenge for 2 h as described above (Fig. 8A). Exposure to Seco A followed by T09 increased the expression of *IL6* (Fig. 9A) and *IL8* (Fig. 9B) compared with the DMSO-treated control. Additionally, individual O_3-derived oxysterol
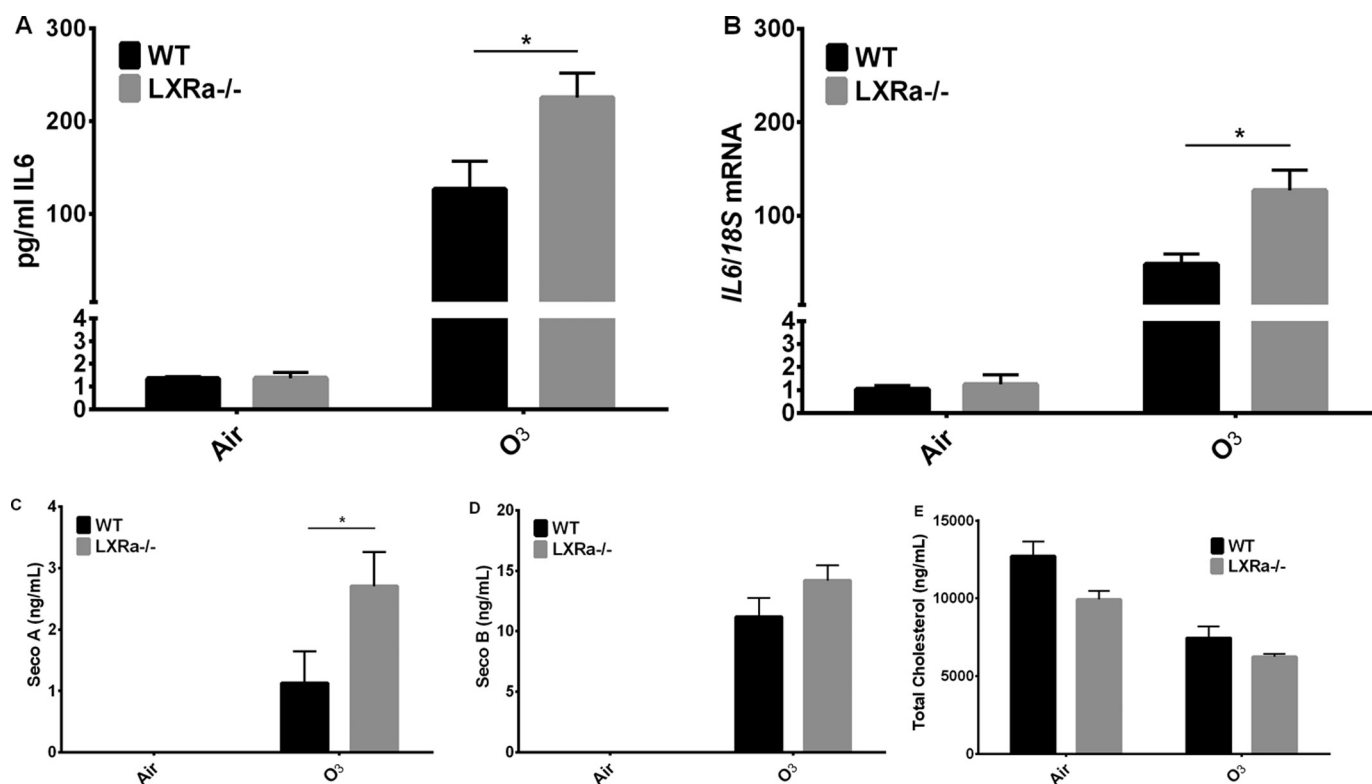
FIGURE 5. **IL6 expression and production in the lung of O$_3$-exposed LXRα-deficient mice.** Wild type (*WT*) and LXR-$\alpha^{-/-}$ female mice were exposed to filtered air (*Air*) or 2 ppm O$_3$ for 3 h. Mice were necropsied 6 h after start of exposure. *A*, bronchoalveolar lavage was collected and evaluated for IL6 cytokine concentrations by ELISA. *B*, after necropsy, lung tissues were collected for RNA isolation and evaluated for gene expression of IL6 and 18S. Bronchoalveolar lavage was also evaluated for total Seco A (*C*), total Seco B (*D*), and total cholesterol (*E*). Data were presented as means ± S.E. Statistical analysis was performed with Mann-Whitney test comparing LXR-$\alpha^{-/-}$ to WT, *, $p < 0.05$, $n = 5$ animals per group.

species significantly increased the NF-κB activity compared with the DMSO control (Fig. 9*C*), suggesting that O$_3$-derived oxysterols enhance pro-inflammatory pathways.

Discussion

Despite a large body of research on O$_3$-induced toxicity and adverse health effects, the biochemical and cellular signaling cascades induced by O$_3$ exposure in the human airways are not fully understood. O$_3$ is a known oxidant of the macromolecules in the airway-lining fluid, and the formation of many oxidized lipid products has been previously described along with their biochemical effects. For example, instillation of 5β,6β-epoxy-cholesterol (β-EpCh) and 1-palmitoyl-2-(9′-oxo-nonanoyl)-glycerophosphocholine, which are both formed during O$_3$ exposure, causes neutrophilic influx, which in turn was regulated by class A scavenger receptors, known to bind oxidized lipids (3). Ozonization of phospholipids generates products with strong pro-inflammatory effects (8, 9). Additionally, O$_3$ is known to react with lung surfactant proteins, modifying and inhibiting their normal biological functions (34–36). O$_3$-induced oxidized cholesterol products, however, have only partially been described in their effects on the biological properties of the human airway. Through this study, our results address the knowledge gap between O$_3$-induced cholesterol oxidation in the airway and downstream cellular signaling events. Our data demonstrate that O$_3$-derived oxysterols can form lipid-protein adducts with cellular signaling molecules, revealing a new paradigm that lipid-protein adduct formation provides a

central mechanism for O$_3$-derived oxidized lipids to modify cellular responses.

Lipid protein adduction as a means to alter normal signaling has been shown to occur during exposure to other oxidative stressors, including the free radical-induced formation of 4-hydroxynoneal (37, 38). Although formation of oxysterols following exposure to O$_3$ has been shown before (28, 35), whether and how these O$_3$-derived oxysterols can form oxysterol-protein adducts in the context of O$_3$ exposure in the human airway has not been examined. Assays based on "click" cyclo-addition methods make it possible to visualize protein-lipid adducts via immunostaining and to determine protein adductions with specific signaling molecules, thus providing novel insight into the mechanisms behind O$_3$-induced adverse health effects (39). Using this approach, our results demonstrate the formation of oxysterol-protein adducts in airway epithelial cells as a result of exposure to O$_3$. The synthetic O$_3$-derived oxysterol Seco A has previously been described as a highly reactive ozonolysis product capable of adducting with the lysine amino acid residues on various proteins (29). Throughout our study, we determined that O$_3$-derived oxysterols, including Seco A, can effectively form adducts with proteins LXR-α, LXR-β, and PPAR-γ, which all regulate lipid metabolism (40, 41). Additionally, supplementation with alkynyl-tagged cholesterol reveals that in the human airway exposure to O$_3$ generates reactive oxysterols capable of forming adducts with the LXR-α and HSP90 proteins. The comparatively diffuse band observed in Fig. 7*D* and quantita-
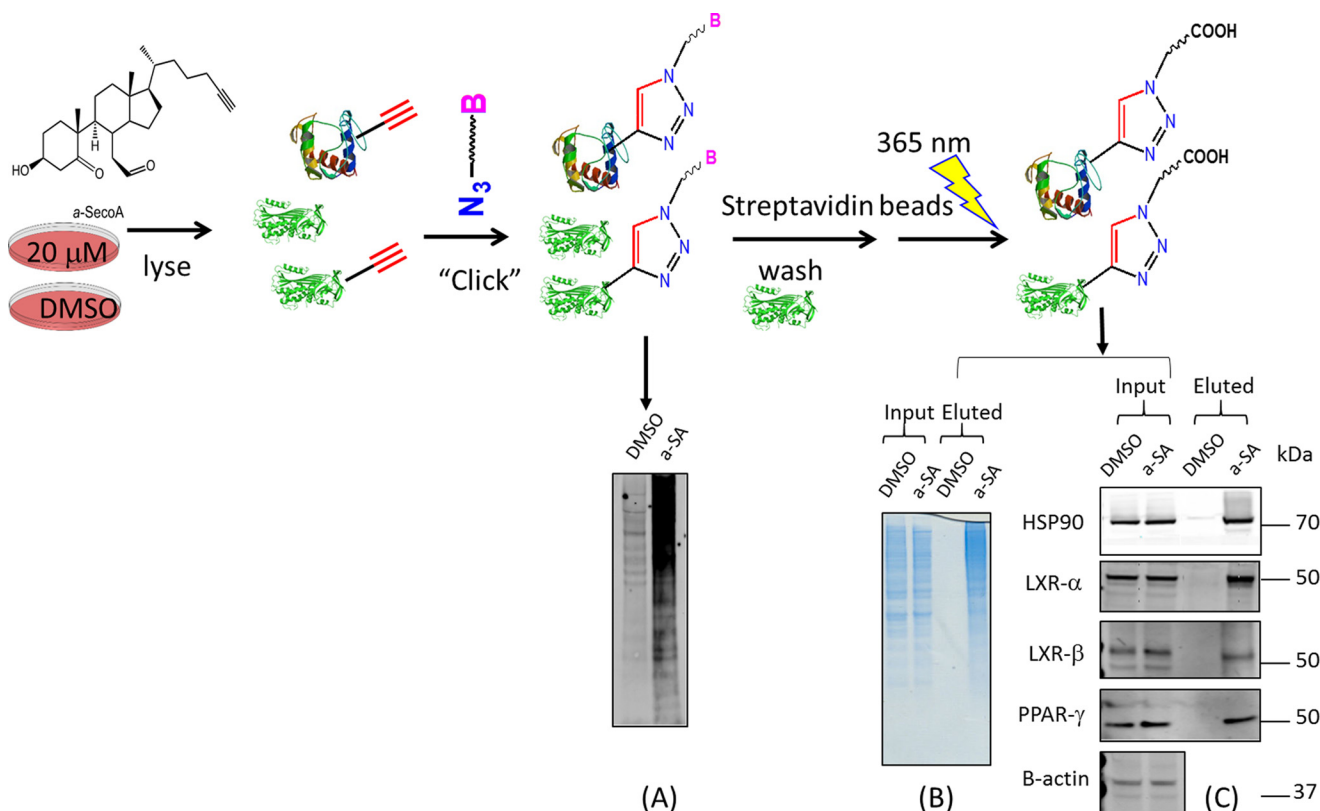
FIGURE 6. **Simplified steps of protein catch and photo-release using *a*-Seco A probe in 16 HBE cells.** Supplementation with *a*-Seco A (20 μM) in 16HBE cells for 4 h at 37 °C followed by cell lysis and click reaction to introduce biotin for immunoaffinity purification. A single aliquot was taken to probe the extent of alkyne labeling via biotin-streptavidin interaction. The rest of the clicked cells were immobilized onto streptavidin beads to catch only adducted proteins and remove un-adducted proteins. Subsequent photo-release permitted us to collect adducted proteins. *A*, IRDye® 800CW streptavidin visualization exhibits the extent of protein labeling with *a*-Seco A. *B*, SDS-polyacrylamide gel of photo-released proteins. An equal amount of total protein was loaded. The *a*-Seco A-treated cells (*right 2 lanes*) exhibited significant protein adduction compared with the input lanes (*left 2 lanes*). *C*, selective antibody analyses indicate adduction on HSP90, LXR-α, LXR-β, and PPAR-γ proteins. Anti-actin of the input lane provides another confirmation of equal loading. Representative blots are from three separate experiments ($n = 3$).

tively analyzed in Fig. 7*E* is most likely indicative of a heterogeneous mixture of O_3-derived oxysterols being formed that can adduct LXR and of a variety of post-translational modifications to LXR-α in addition to *a*-Seco A adduction resulting in a mixture of proteins recognizable by the anti-LXR-α antibody. Hence, data presented here reveal a novel biochemical mechanism involving the conversion of cellular cholesterol by O_3 into reactive oxysterol species, a process that results in the adduction of key proteins and modification of cellular signaling.

The formation of adducts between O_3-derived oxysterols and LXR provides a model signaling mechanism, which results in modifications of airway inflammatory and cholesterol homeostasis signaling. Endogenous oxysterols are known to be formed during normal cholesterol regulation and metabolism. These compounds play a role in normal LXR activation, promoting cholesterol homeostasis. Mouse model systems with LXR and cholesterol efflux deficiencies have higher cholesterol accumulation, potentiated atherosclerosis, and are more susceptible to systemic infection (42). These effects occur partially via the endogenous oxysterol-induced activation of LXR and transcriptional activation of genes such as *ABCA1*, which mediate cholesterol shuttling and ultimately packaging into HDL (43, 44). In contrast, our data show that in human bronchial epithelial cells, O_3 exposure decreases the expression of *ABCA1*, suggesting that O_3 or its oxidation products have an

inhibitory effect on the transcriptional activation of *ABCA1*. Decreased *ABCA1* expression and subsequent decreased cholesterol efflux may result in accumulation of intracellular cholesterol leading to dyslipidemia and propagation of respiratory, metabolic, and cardiovascular health problems (13, 45). Whether the observations related to O_3-induced suppression of *ABCA1* expression affect systemic cholesterol metabolism and potentially contribute to the enhanced atherosclerosis and cardiovascular events associated with O_3 exposure remain to be established. In addition to cholesterol homeostasis, previous studies have indicated that normal LXR activation is necessary for immune health. LXR activation by synthetic agonists leads to decreased neutrophil recruitment and increased bacterial burden, indicating that LXR activation balance contributes to host immune defense (46). Recent studies also suggest that LXR agonists show therapeutic promise in treating lung disorders such as dyslipidemia and asthma (43, 47, 48). Furthermore, our data show that O_3 exposure of LXR$\alpha^{-/-}$ mice results in enhanced pro-inflammatory response, indicating the importance of normal LXRα activity to regulate O_3-induced inflammation (Fig. 5, *A* and *B*). The enhanced concentration of O_3-derived oxysterols in the bronchoalveolar lavage sampled from the LXR$\alpha^{-/-}$ mice further link airway cholesterol ozonolysis and LXRα activity. It is interesting that overall cholesterol levels were reduced in these mice exposed to O_3, a change we did not
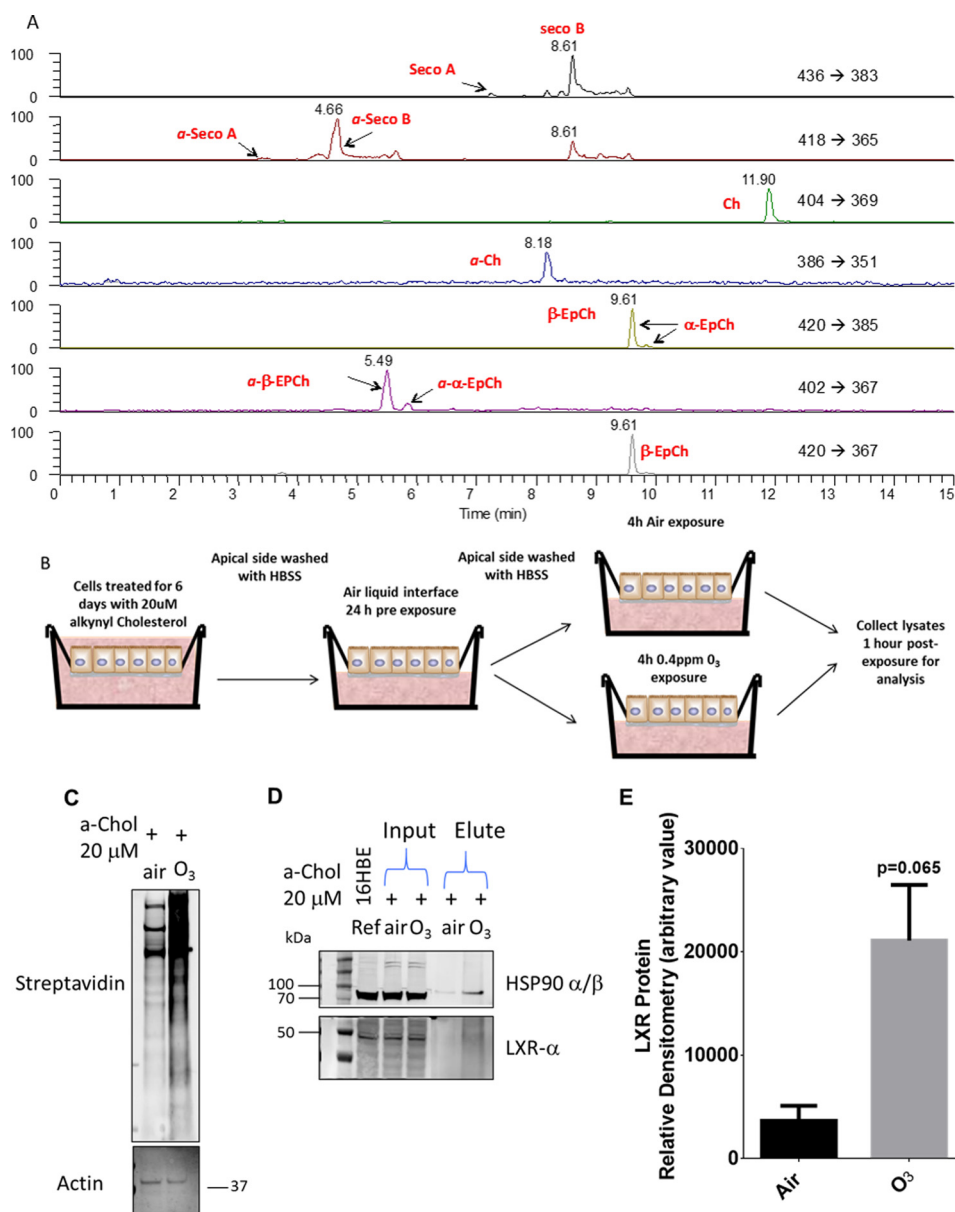
FIGURE 7. **Protein adduct formation is observable in 20 μM *a*-Chol-supplemented 16HBE cells exposed to O₃.** Following *a*-Chol supplementation (20 μM), apical medium was removed, and the cells were exposed to clean air or 0.4 ppm O₃ for 4 h. Cells were harvested after 1 h of postincubation. *A,* lipids were extracted as described in experiment. LC-selected reaction monitoring profile demonstrates that *a*-cholesterol was incorporated into the cells and generated ozone-derived oxysterols as those of endogenous cholesterol. *B,* schematic depicting *a*-Chol supplementation prior to O₃ exposure. *C,* cells harvested in lysis buffer containing inhibitors were clicked with azido-biotin. IRDye® 800CW streptavidin probe displays significant extent of protein adduction upon O₃-exposed cells, whereas the background levels of adduction with air-exposed cells were observed. Anti-actin is served as a loading control. *D,* HSP90 and LXR-α Western blots of click and photo-released proteins. 16HBE cell lysates were loaded as a positive control. *E,* relative densitometry analysis of LXR-α protein levels from three separate immunoblots (*n* = 3).

observe in our human subjects. Taken together, LXR dysfunction caused by O₃-derived oxysterols may contribute to enhanced respiratory inflammation and adverse cardiovascular health effects in humans exposed to O₃.

Based on our observation of adduct formation between O₃-derived oxysterols and LXR, we hypothesize that electrophilic O₃-induced oxysterols and their derived lipid protein adducts inhibit cholesterol signaling pathways that are normally activated by endogenous oxysterols. Our data in Fig. 8*E* show that O₃-derived oxysterols alone are not themselves potent activators of LXR but that treatment with Seco A prior to activation of LXR by the agonist T09 reduces T09-induced

LXRE activation as well as expression of *ABCA1, FASN,* and *SREBP1.* These data suggest that Seco A-induced adduct formation with LXR may prevent its activation with known agonists, such as T09, or endogenous oxysterols, such as 27-hydroxycholesterol (49). Our previous studies have demonstrated that Seco A readily adducts to nucleophilic lysine amino acid residues in human serum albumin and other proteins, and we hypothesize a similar binding site in LXR (29). LXR contains eight lysines in a ligand binding domain (amino acids 215–434) that are capable of binding both oxysterol and T09 ligands (14). Based on our results, we propose that O₃-derived oxysterols block T09-mediated LXR activation either by non-competitive
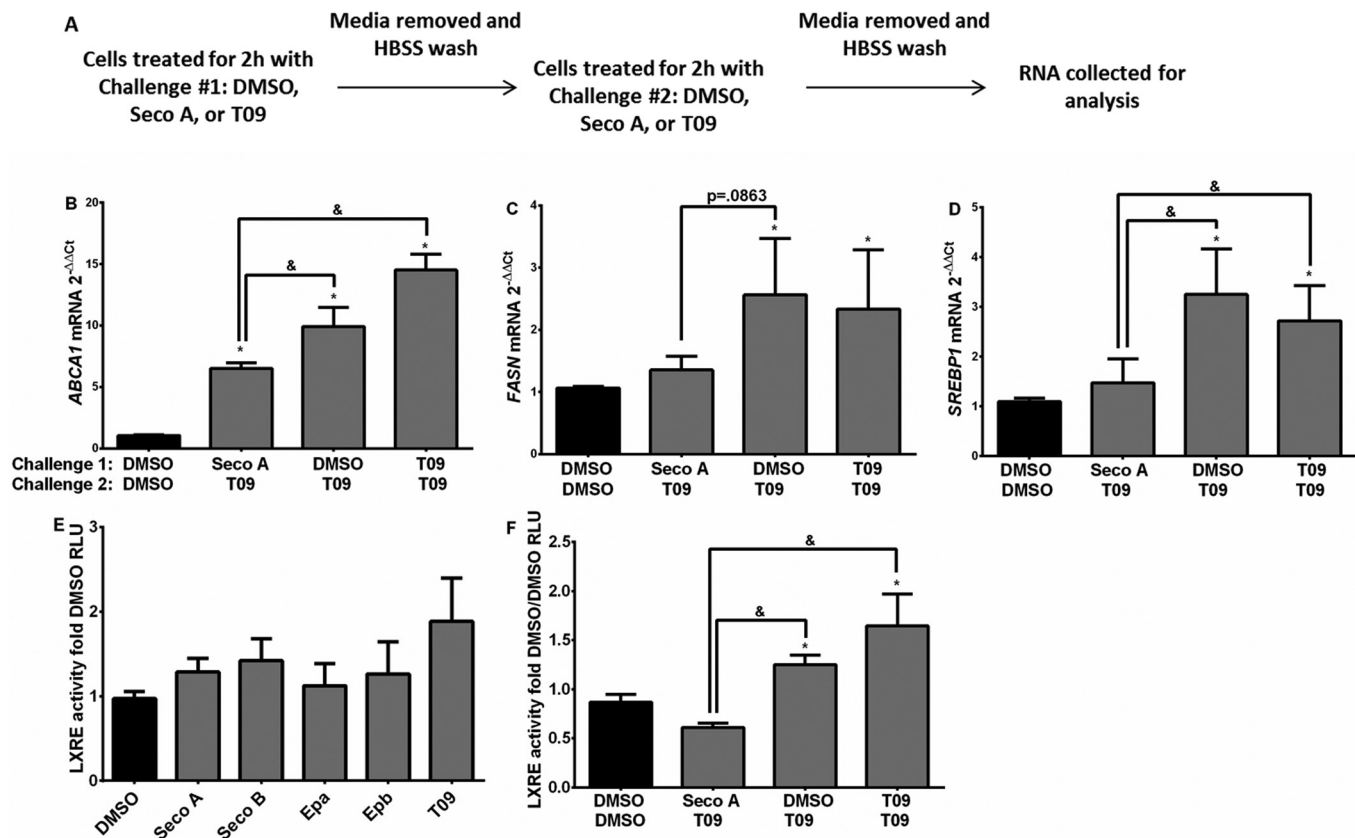
FIGURE 8. **Seco A-altered cholesterol efflux pump gene expression when treated with Seco A and the T09 LXR agonist in sequence.** *A*, experimental design depicting how 16HBE cells were challenged for 2 h to 20 μM Seco A, 10 μM T09, or DMSO control for first challenge; media were removed and followed by 2 h of second challenge. Samples were evaluated for *ABCA1* (*B*), *FASN* (*C*), and *SREBP1* (*D*) gene expression. LXRE activity was measured in relative luciferase units (*RLU*) compared with the respective vehicle control in the individual oxysterol challenges at 20 μM for 4 h (*E*) and sequential treatment in 16HBE cells (*F*). Data are presented as mean $\pm$ S.E. of fold change compared with the DMSO control. Statistical analysis was performed with a one-way ANOVA and Fisher's LSD post hoc comparison test, * significantly different from the DMSO control; & significantly different from the indicated conditions, $p < 0.05$, $n = 3$.
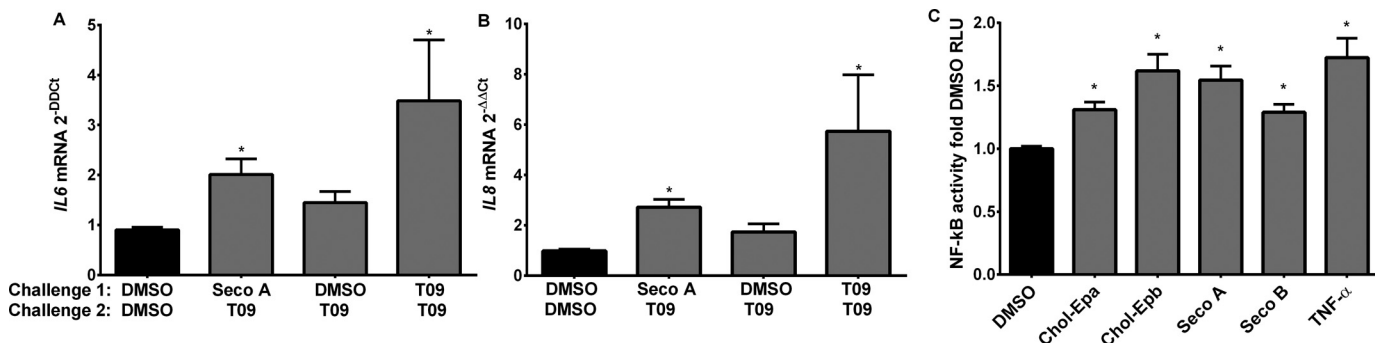
FIGURE 9. **Oxysterol altered inflammatory signaling.** *IL6* (*A*) and *IL8* (*B*) gene expression in sequential challenge of 2 h with first challenge followed by another 2 h of second challenge on 16HBE cells exposed to 20 μM of Seco A, 10 μM T09, or DMSO control on collagen-coated plates. *C*, relative light units of NF-κB promoter reporter activity in 16HBE cells exposed to 20 μM of various oxysterols, 20 ng/ml TNF-α, or DMSO negative control for 4 h on collagen-coated plastic. Data are presented as mean $\pm$ S.E. of fold-change compared with the DMSO control. Statistical analysis was performed with a one-way ANOVA and Fisher's LSD post hoc comparison test, *, $p < 0.05$, $n = 3$.

binding to the same site or by modifying the LXR structure to inhibit normal ligand binding. Additional studies are necessary to clarify the nucleophilic peptide site of O_3-derived oxysterol LXR adduct formation.

In contrast to expression of *ABCA1*, expression of *IL6* and *IL8* as well as activation of NF-κB were enhanced by exposure to Seco A and other O_3-derived oxysterols. O_3 is known to activate NF-κB leading to increased transcription of inflammatory cytokines such as *IL6* and *IL8* (31, 50, 51). Similarly, other lipid ozonization products have been shown to activate *IL6* and *IL8*

in human airway epithelial cells (9). Our study shows that O_3-derived oxysterols enhance activation of NF-κB and potentiate the transcription of *IL6* and *IL8*. LXR signaling has been shown previously to have an inhibitory effect on NF-κB and inflammatory signaling in epithelial cells (52, 53), making it a reasonable target for O_3-derived oxysterol-induced modification of inflammatory signaling. All the O_3-derived oxysterol species we tested increased NF-κB activity, revealing that in their presence airway epithelial cells may experience increased inflammatory signaling leading to adverse health effects. In the

experiments using sequential stimulation with Seco A and T09, stimulation with Seco A alone, regardless of the secondary stimulus, increases *IL6* and *IL8* expression, indicating that O_3-derived oxysterols potentiate the transcription of pro-inflammatory cytokines. In addition to directly activating the NF-κB pathway, we hypothesize that this effect may be linked to inactivation of LXR. Activation of LXR induces a number of anti-inflammatory responses, marked by inhibition of NF-κB activity and decreased production of pro-inflammatory mediators (54). Previous rodent studies show the use of LXR agonists to inhibit NF-κB activation to reduce lung injury and inflammation after hemorrhage and resuscitation (55). In this role, LXR is not recruited to LXR response elements in genes related to lipid metabolism, but it does participate in a transrepression mechanism of NF-κB, resulting in inhibition of inflammatory genes such as *IL6* (42, 56, 57). LXR activity is controlled by a post-translational SUMOylation modification and interaction with nuclear receptor co-repressors, reducing NF-κB activity (58–60). The proposed SUMOylation occurs at the lysine residues of LXR ensuring retinoid X receptor dimerization and nuclear translocation (60). Thus, lipid-adduct formation at or near these lysine residues may prevent SUMOylation of LXR, interaction with co-repressors, and consequently activation of NF-κB. This proposed signaling mechanism provides a link between our observed O_3-derived oxysterol-induced changes to LXR signaling and a model for O_3-induced NF-κB activation.

To enhance our understanding of O_3-induced cardiovascular events and atherosclerosis, the biochemical mechanisms involving O_3-derived oxysterols, adduct formation with LXR, and reduced *ABCA1* expression that are reflected in systemic changes need to be examined. Interestingly, epidemiological studies repeatedly demonstrate the beneficial effects of cholesterol-modifying drugs, such as statins, on air pollutant-induced adverse health effects (61–65). Yet the mechanisms mediating these effects are unknown and have often been ascribed to the anti-inflammatory effects of statins. The findings presented in this study provide an additional explanation for the beneficial effects of statins on the response to inhaled O_3. Therapeutic treatment with lipid-targeting agents such as statins may reduce cholesterol availability in the airways, thus reducing oxysterol formation, and lead to changes in O_3-induced inflammation.

Collectively, our results suggest that reactive oxysterols formed in the airways following O_3 exposure interact with the LXR signaling pathway, alter expression of genes that regulate cholesterol efflux, fatty acid synthesis, and cholesterol regulation, and enhance pro-inflammatory signaling pathways known to be associated with O_3 exposure. Our findings indicate that cholesterol availability is paramount to the formation of O_3-derived oxysterols in the airway and may provide a novel therapeutic target to reduce the adverse effects associated with ambient O_3 exposure. In addition to LXR examined here, other proteins are also likely targets for adduction by O_3-derived oxysterols and warrant future study into their implications in O_3-induced airway inflammation. Together, our data describe a novel mechanistic concept linking O_3 reactions with cholesterol moieties in the human airway and its impact on health outcomes. Our data also highlight the use of samples derived

from human *in vivo* O_3 exposure as well as primary HBECs and 16HBE cells to provide clinical and biological relevance for O_3-derived oxysterol and their role in O_3-induced inflammation in the human airway.

Experimental Procedures

Reagents—Alkynyl probes were synthesized following the procedures published elsewhere (29, 32). DTT and iodoacetamide were purchased from Sigma. Streptavidin beads were purchased from GE Healthcare. The following reagents were purchased from their respective companies: 10% NuPAGE Novex BisTris® precast mini gel (Invitrogen); PVDF membrane and Simply Blue (Bio-Rad); IRDye® 800CW streptavidin (925-32230, Li-Cor, Lincoln, NE); Blocking buffer (Rockland, Gilbertsville, PA, or Odyssey Blocking buffer, Li-Cor); and sequencing grade trypsin (Promega V5111, Madison, WI). Antibodies of HSP90, LXR-β, PPAR-γ, and actin were from Santa Cruz Biotechnology (Dallas, TX), and LXR-α was purchased from Abcam® (Cambridge, MA).

Cell Culture—16HBE14o (16HBE) cells, an SV-40-transformed human bronchial epithelial cell line, were a gift from Dr. D. C. Gruenert (University of California at San Francisco). 16HBE cells were plated on fibronectin-coated (LHC Basal Medium (Life Technologies, Inc.), 0.01% BSA (Sigma), 1% Vitricol (Advanced Bio Matrix, San Diego), and 1% human fibronectin (BD Biosciences)) 0.4-μm Transwell® plates (Costar, Corning, NY) and grown submerged in minimal essential media (Gibco) with 10% FBS, 1% penicillin-streptomycin, and 1% L-glutamine (Life Technologies, Inc.) until confluent for 6 days and 1 day at air-liquid interface before use. Primary HBECs were obtained from healthy donors in collaboration with the Environmental Protection Agency (EPA) using a protocol approved by the University of North Carolina at Chapel Hill Institutional Review Board (Chapel Hill, NC), as described previously (66) The HBECs were cultured in PneumaCult medium for 21 days to differentiate according to previously described methods (67, 68).

In Vitro O_3 Exposure—Cultures at the air-liquid interface were exposed to filtered air or 0.4 ppm O_3 for 4 h in exposure chambers operated by the United States EPA, as described previously (69). The dose was selected for maximal innate immune response to O_3 with minimal cytotoxicity and has been used previously by our group (68). At 1 or 24 h after exposure, apical sides of all cultures were washed with 100 μl of Hanks' balanced salt solution (HBSS) (Life Technologies, Inc.) and saved for LC-MS analysis. The remaining cells were collected in 200 μl of PBS, centrifuged at 500 $\times$ g for 5 min, and stored at -80 °C until LC-MS analysis.

In Vivo Exposure of Healthy Volunteers to O_3—Written informed consent was provided by each participant. Healthy volunteers were randomly exposed to air and (in a separate exposure) 0.3 ppm O_3 for 2 h with exercise, with a minimum 2-week separation between exposures in collaboration with the EPA using a protocol approved by the University of North Carolina Chapel Hill Institutional Review Board, as described previously (70). Bronchoscopy was performed 1 and 24 h after exposure. Cell-free BALF was stored at -80 °C pending analysis (30).

Oxysterol and Lipid-Protein Adducts

Real Time qPCR—Total RNA was isolated from 16HBEs and HBECs with the use of the Pure Link RNA mini kit (Life Technologies, Inc.). First strand cDNA preparation and real time qPCR were performed as described previously (71, 72). The following primers and probes for *ABCA1*, *ABCG1*, *FASN*, *SREBP1*, and *ACTB* were commercially available (Applied Biosystems, Foster City, CA) and were prepared in-house: human *IL8*, 5′-FAM-CCTTGGCAAAACTGCACCTTCAC-TAMRA-3′ (probe), 5′-TTGGCAGCCTTCCTGATTTC-3′ (sense), and 5′-TATGCACTGACATCTAAGTTCTTTAGCA-3′ (antisense); and *IL6*, 5′-FAM-CCAGCATCAGTCCCAAGAA-GGCAACT-TAMRA-3′ (probe), 5′-TATGAAGTTCCTCTC-TGCAAGAGA-3′ (sense), and 5′-TAGGGAAGGCCGTG-GTT-3′ (antisense). Differences in expression were determined with the $\Delta\Delta Ct$ method and *ACTB* for normalization. Briefly, threshold cycle (*Ct*) value for the housekeeping gene *ACTB* was subtracted from the *Ct* value for the gene of interest to determine the ΔCt value. For each pairwise set of samples to be compared, the difference in ΔCt values between the two samples were calculated for the genes of interest to determine the ΔCt value. The fold-change in gene expression was calculated as $2^{-\Delta\Delta Ct}$.

Sterol Profiling Using PTAD Derivatization and LC-selected Reaction Monitoring Analysis—Cells were scraped into 400 μl of cold PBS. 200 μl of the 400 μl were taken and internal standards added (13 ng for d_7-7-dehydroxycholesterol (d_7-7-DHC), 97 ng for $^{13}C_3$-desmosterol, 99 ng for $^{13}C_3$-lanosterol, and 342 ng for d_7-cholesterol/sample), 10 μl of butylated hydroxytoluene (BHT)/triphenylphosphine (TPP) solution (2.5 mg of TPP and 1 mg of BHT in 1 ml of MeOH), 400 μl of 1% NaCl, and 500 μl of Folch solution (2:1 = CHCl$_3$/MeOH). Cells and standards were vortexed vigorously and centrifuged at 3099 $\times$ g for 5 min. CHCl$_3$ layer was removed and added to PTAD-predeposited tube (200 μg/tube). The sample tubes were vortexed and analyzed by LC-MS using the following conditions: 10 μl was injected onto the column (Acquity UPLC BEH C18, 1.7 μm, 2.1 $\times$ 50 mm) with 100% MeOH (0.1% acetic acid) mobile phase for a 1 min runtime at a flow rate of 300 μl/min. The monitored transitions included 7-DHC *m/z* 560 $\rightarrow$ 365, d_7-7-DHC *m/z* 567 $\rightarrow$ 372, desmosterol *m/z* 592 $\rightarrow$ 365, $^{13}C_3$-desmosterol *m/z* 595 $\rightarrow$ 368, lanosterol *m/z* 634 $\rightarrow$ 602, $^{13}C_3$-lanosterol *m/z* 637 $\rightarrow$ 605 with retention times of 0.8, 0.5, and 0.6 min, respectively.

Oxysterol Extraction from 16HBE or HBEC Cells—To the cell pellets 10 μl of *a*-Chol (25 ng/μl), 500 μl of NaCl (0.9%), 10 μl of TPP and BHT (25 mg of TPP and 10 mg of BHT in 10 ml of MeOH), and 1 ml of Folch solution (2:1 = CHCl$_3$/MeOH) were added. The mixture was mixed vigorously by vortex for 2 min and separated by centrifugation with 2300 $\times$ g for 3 min. The collected organic layer (bottom layer) was evaporated to dryness in a SpeedVac^{TM} concentrator and resuspended in 100 μl of MeOH for LC-MS analysis.

Oxysterol Extraction from Cell-free BALF—To 1 ml of BALF 10 μl of alkynyl-Seco B (*a*-Seco B) (50 ng/μl), 1 ml of NaCl (0.9%), 10 μl of TPP and BHT (25 mg of TPP and 10 mg of BHT in 10 ml of MeOH), 2 ml of MeOH, and 3 ml of iso-octane were added. The mixture was vortexed vigorously for 2 min and separated by centrifugation. The collected organic layer was evap-

orated to dryness in a SpeedVac^{TM} concentrator and resuspended in 100 μl of MeOH for LC-MS analysis.

LC-MS Analysis—The resuspended samples were chromatographed by reverse phase-HPLC using a UPLC BEH C18 column (1.7 μm, 2.1 $\times$ 100 mm) in Waters Acquity UPLC system equipped with an autosampler (Waters, Milford, MA) and either electrospray ionization or atmospheric pressure chemical ionization in positive ion mode. For electrospray ionization, the oxysterols were separated by 95% solvent B in an isocratic method with a flow rate of 200 μl/min, and the mobile phase solvents consisted of 2 mM NH$_4$OAc (solvent A) in water and 2 mM NH$_4$OAc in MeOH (solvent B). The injection volume was 10 μl using a partial loop with needle overfill mode. MS detections were done using a TSQ Quantum Ultra tandem mass spectrometer (ThermoFisher, Waltham, MA), and data were acquired and analyzed using a Thermo Xcalibur^{TM} 2.2 software package. The cholesterol and oxysterols form [M + NH$_4$]$^+$ ions in positive ion mode (10). The transitions monitored were *m/z* 436 $\rightarrow$ 383 for Seco A/B, *m/z* 418 $\rightarrow$ 365 for *a*-Seco A/B, *m/z* 404 $\rightarrow$ 369 for Chol, *m/z* 386 $\rightarrow$ 351 for *a*-Chol, *m/z* 420 $\rightarrow$ 385 for α/β EpCh, and *m/z* 402 $\rightarrow$ 367 for α/β *a*-EpCh. For atmospheric pressure chemical ionization, 95% MeOH in H$_2$O containing 0.01% acetic acid was used as a mobile phase. The cholesterol and oxysterols form [M + H]$^+$ ions in positive ion mode. The transitions were *m/z* 369 $\rightarrow$ 369 for Chol, *m/z* 383 $\rightarrow$ 383 for Seco A/B, *m/z* 351 $\rightarrow$ 351 for *a*-Chol, and *m/z* 385 $\rightarrow$ 385 for α/β EpCh. The transitions of cholesterol and cholesterol esters were *m/z* 365 $\rightarrow$ 365 monitored by HPLC-MS following the method described elsewhere (73). The amount of the cholesterol esters were found to be less than 2% of free cholesterol in the cells studied.

Cytokine Analysis—Concentration of IL6 and IL8 in the apical wash of 16HBE cells exposed to O$_3$ was determined by enzyme-linked immunosorbent assay (ELISA) according to the manufacturer's instructions (BD Biosciences).

Western Blotting—Cell lysates from 16HBE cells exposed to air/O$_3$ or O$_3$-derived oxysterols were separated by 10% SDS-PAGE and transferred to nitrocellulose. Proteins were detected using specific antibodies (Santa Cruz Biotechnology) to ABCA1 (1:500) or β-actin (1–2000), which served as a loading control. Antigen-antibody complexes were incubated with horseradish peroxidase-conjugated secondary antibody and were detected using chemiluminescence.

Murine Whole Body O$_3$ Exposure, BAL, Cytokine and RNA Analysis—C57BL/6J (WT) female mice, 8–12 weeks old and weighing 15–20 g, were purchased from The Jackson Laboratory (Bar Harbor, ME). LXR$\alpha^{-/-}$ female mice, 8–12 weeks old and weighing 15–20 g, originally a kind gift from Dr. David Mangelsdorf, were bred in-house and backcrossed >8 generations onto a C57BL/6 background before use. All experiments were performed in accordance with the Animal Welfare Act and the United States Public Health Service Policy on Humane Care and Use of Laboratory Animals after review by the Animal Care and Use Committee of the NIEHS, National Institutes of Health. Mice were placed in stainless steel wire exposure chambers inside a Plexiglas chamber and exposed to filtered air or O$_3$ for 3 h at a dose of 2 ppm. O$_3$ was generated by directing 100% oxygen through an ultraviolet light generator and mixed with

a humidified air supply to the chamber. Temperature and humidity of chamber air were monitored continuously, as was the O_3 concentration with a Teledyne T400 ultraviolet light photometer. BALF was collected immediately following sacrifice, and cell counts were performed as described previously (74). Protein analysis was performed using BCA protein assay (Pierce). Cytokine analysis was performed using a Bioplex assay for IL6 on the BALF (Bio-Rad). After necropsy, lung tissue samples were snap-frozen in liquid nitrogen and stored at -80 °C until RNA isolation. RNA was extracted and cDNA transcribed (Applied Biosystems, Foster City, CA). 50 ng of cDNA was used for qPCR for IL6 (Mm00446190_m1; Applied Biosystems) and endogenous 18S (4319413) (Applied Biosystems). *Ct* values were determined using ABI 7500 Real Time PCR System with SDS software version 1.3.1. Change in expression was calculated using the $2^{-\Delta\Delta Ct}$ method normalized to 18S expression and expressed as fold-change compared with the control group.

Cell Culture and Whole Cell Labeling with a-Seco A in 16HBE—16HBE cells were plated 2×10^6 in 10-cm plates using the conditions described above and then allowed to settle and grow for 24 h. The cells were then incubated in the presence of *a*-Seco A (20 μM) in reduced FBS (2%) MEM for 4 h. Cells were harvested in lysis buffer (50 mM HEPES, 150 mM NaCl, 0.1% Triton X-100, pH 7.0) containing protease inhibitors (Sigma P8340) on ice. The lysate was cleared by centrifugation at $10,000 \times g$ for 10 min at 4 °C to remove cellular debris. The total protein concentration was determined using standard BCA assay (Pierce, ThermoFisher) for further click reaction.

Cell Culture and Whole Cell Labeling with a-Cholesterol Followed by Ozone Exposure in Human Bronchial Epithelial Cells (16HBE)—16HBE cells were grown in 24-mm transwells submerged in MEM with reduced FBS containing 20 μM *a*-Chol for 6 days. The apical media were removed 24 h before exposure. Next, the plate was exposed to filtered air or O_3 (0.4 ppm) for 4 h and allowed to continue for an additional 1 h of incubation without O_3 (1 h postincubation). Cells were harvested in 300 μl of lysis buffer/well on ice, and all wells were then combined for each condition. The lysate was cleared by centrifugation at $10,000 \times g$ for 10 min at 4 °C to remove cellular debris. The total protein concentration was determined using standard BCA assay (Pierce, ThermoFisher) for further click reaction.

Click Biotinylation of a-Seco A/a-Oxysterols Adducted Proteins in 16HBE and Streptavidin Affinity Purification—1 ml of cell lysates (2 mg/ml) was reduced with sodium borohydride, 5 mM final concentration, for 1 h on ice to stabilize the adducts. Excess sodium borohydride was deactivated by acidification of the mixture by adding 1 M HCl. Subsequently, all click reagents were added to the reduced cell lysates, including the photo-cleavable azido-biotin (39) (0.2 mM final concentration, tris(3-hydroxypropyltriazoylmethyl)amine (75) (0.2 mM), CuSO$_4$ (1 mM), and sodium ascorbate (1 mM)), and the reaction mixture was vortexed and allowed to react at room temperature for 1 h. 50 μl of the reaction mixture was saved for streptavidin visualization. The rest was precipitated using cold methanol (3:1 = MeOH/H$_2$O, v/v) to remove excess biotin linker. The precipitated protein pellets were reconstituted in 1 ml of 0.1% SDS in PBS, including 200 μl of streptavidin (GE Healthcare) slurry. The slurry was rotated in the dark for 2 h at room temperature

to capture the adducted proteins. After 2 h, the tube was spun at $95 \times g$ for 1 min, and the supernatant was removed (flow-through). The beads were then washed with 1 ml of 1% SDS (two times), 4 M urea (two times), and 1 M NaCl (two times, and 25 mM ammonium bicarbonate (AMBIC, two times), respectively. The slurry was transferred to a 0.2-μm cellulose acetate spin filter (Costar) in 500 μl of 25 mM AMBIC and spun at $95 \times g$ for 1 min. The slurry was resuspended with AMBIC and photolyzed under hand-held UV light (365 nm) for 2 h with gentle stirring at room temperature. The spin filter was spun at $95 \times g$ for 1 min to recover photo-released proteins. The beads were washed twice with 500 μl of 25 mM AMBIC, and the combined filtrates were evaporated to dryness in a SpeedVac^{TM} concentrator.

Visualization of Biotinylated Proteins Adducted with a-Seco A/a-Oxysterols—The saved 50 μl of click reaction mixture was mixed with SDS sample loading buffer and resolved using 10% NuPAGE Novex BisTris® gel (Invitrogen). The proteins were electrophoretically transferred to a polyvinylidene difluoride (PVDF) membrane (Bio-Rad) and probed with IRDye® 800CW streptavidin (Li-Cor). The extent of adduction was visualized using Odyssey Infrared Imaging System^{TM}.

Immunoblotting Analysis of Photo-released Proteins—The photo-released and dried proteins were reconstituted in 70 μl of PBS, 25 μl of LDS buffer, and 5 μl of 1 M DTT and resolved by 10% NuPAGE Novex BisTris® gel and then transferred to PVDF membrane. The transferred proteins were incubated with antibodies of HSP90 (anti-rabbit, Santa Cruz Biotechnology), LXR-α (anti-rabbit, Abcam®), LXR-β (anti-rabbit, Santa Cruz Biotechnology), or PPAR-γ (anti-mouse, Santa Cruz Biotechnology) (1:1000) overnight in the cold room at 4 °C. Alexa Fluor 680®-labeled secondary anti-rabbit or anti-mouse was used to detect target proteins. Immunoreactive proteins were visualized using Odyssey Infrared Imaging System^{TM} (Li-Cor).

Modification of Gene Expression by Sequential Seco A-T09 Challenges—16HBE cells were grown submerged in MEM and repeatedly challenged with 20 μM Seco A, 10 μM T09 or DMSO in a crossover design. Briefly, cells were challenged with the first stimulus for 2 h, washed with HBSS, and challenged again with either 20 μM Seco A, 10 μM T09 or DMSO for 2 h. The cells were washed again with HBSS, and RNA was collected for analysis as described above.

NF-κB and LXRE Promoter Reporter Activity in 16HBE Cells—16HBE cells were transduced with NF-κB-luciferase lentiviral vector at a multiplicity of infection of 5 and were cultured for 7 days (76). To select for transduced cells, the cells were cultured with hygromycin for 9 days to create a stable cell line, which was used for subsequent reporter assays. To assess NF-κB activation, stably transduced 16HBE cells were plated overnight and then treated with α-EpCh, β-EpCh, Seco A, Seco B (all 20 μM), or TNF-α (20 ng/ml, Calbiochem, Billerica, MA) for 4 and 24 h. For the LXRE promoter activity measurement, LXRE-luciferase vector (System Biosciences Inc., San Francisco, CA) was transiently transfected into 16HBE cells and allowed to expand for at least 1 day. The cells were then exposed to individual oxysterols or used in the sequential challenge with Seco A and T09 as described above. Cell lysates were harvested and subjected to Dual-Luciferase assay (Promega, Madison,

WI). Data were normalized to total protein levels and expressed as relative luciferase units.

Statistical Analysis—All *in vitro* data were performed in at least three separate experiments. Data shown are means ± S.E. and significance indicated as $p < 0.05$. See figure legends for further information on the specific statistical analysis used for each experiment.

Author Contributions—A. M. S. conducted the biological experiments, analyzed the results, and summarized the findings in the manuscript. H. Y. K. performed the biochemical analysis and helped with writing the manuscript. W. L. performed the preliminary biochemical analysis. R. N. B. performed preliminary biological experiments and replicate cell culture experiments for this study. M. M. conducted lentiviral transfection assays and luciferase promoter/reporter analysis. K. M. G. and M. B. F. conducted the mouse model exposure experiment, sample acquisition, and analysis. K. E. D. obtained and processed BALF samples for analysis. N. A. P. provided expertise in cholesterol chemistry, conceived the biochemical analysis, and helped write the manuscript. I. J. conceived the idea for the project and wrote and edited the manuscript with A. M. S.

References

1. United States Environmental Protection Agency (2014) National Ambient Air Quality Standards (NAAQS)-Ozone (O3). Office of Air and Radiation, www.epa.gov/naaqs/ozone-o3-air-quality-standards

2. Hollingsworth, J. W., Kleeberger, S. R., and Foster, W. M. (2007) Ozone and pulmonary innate immunity. *Proc. Am. Thorac. Soc.* **4,** 240–246

3. Dahl, M., Bauer, A. K., Arredouani, M., Soininen, R., Tryggvason, K., Kleeberger, S. R., and Kobzik, L. (2007) Protection against inhaled oxidants through scavenging of oxidized lipids by macrophage receptors MARCO and SR-AI/II. *J. Clin. Invest.* **117,** 757–764

4. Kirichenko, A., Li, L., Morandi, M. T., and Holian, A. (1996) 4-Hydroxy-2-nonenal-protein adducts and apoptosis in murine lung cells after acute ozone exposure. *Toxicol. Appl. Pharmacol.* **141,** 416–424

5. Pryor, W. A., Wang, K., and Bermúdez, E. (1992) Cholesterol ozonation products as biomarkers for ozone exposure in rats. *Biochem. Biophys. Res. Commun.* **188,** 618–623

6. Uppu, R. M., Cueto, R., Squadrito, G. L., and Pryor, W. A. (1995) What does ozone react with at the air/lung interface? Model studies using human red blood cell membranes. *Arch. Biochem. Biophys.* **319,** 257–266

7. Kafoury, R. M., Pryor, W. A., Squadrito, G. L., Salgo, M. G., Zou, X., and Friedman, M. (1999) Induction of inflammatory mediators in human airway epithelial cells by lipid ozonation products. *Am. J. Respir. Crit. Care Med.* **160,** 1934–1942

8. Kafoury, R. M., Pryor, W. A., Squadrito, G. L., Salgo, M. G., Zou, X., and Friedman, M. (1998) Lipid ozonation products activate phospholipases A2, C, and D. *Toxicol. Appl. Pharmacol.* **150,** 338–349

9. Kafoury, R. M., Hernandez, J. M., Lasky, J. A., Toscano WAJr, and Friedman, M. (2007) Activation of transcription factor IL-6 (NF-IL-6) and nuclear factor-κB (NF-κB) by lipid ozonation products is crucial to interleukin-8 gene expression in human airway epithelial cells. *Environ. Toxicol.* **22,** 159–168

10. Pulfer, M. K., Taube, C., Gelfand, E., and Murphy, R. C. (2005) Ozone exposure in vivo and formation of biologically active oxysterols in the lung. *J. Pharmacol. Exp. Ther.* **312,** 256–264

11. Murphy, R. C., and Johnson, K. M. (2008) Cholesterol, reactive oxygen species, and the formation of biologically active mediators. *J. Biol. Chem.* **283,** 15521–15525

12. Smith, L. L., and Johnson, B. H. (1989) Biological activities of oxysterols. *Free Radic. Biol. Med.* **7,** 285–332

13. Fessler, M. B. (2008) Liver X receptor: crosstalk node for the signaling of lipid metabolism, carbohydrate metabolism, and innate immunity. *Curr. Signal. Transduct. Ther.* **3,** 75–81

14. Jakobsson, T., Treuter, E., Gustafsson, J. Å., and Steffensen, K. R. (2012) Liver X receptor biology and pharmacology: new pathways, challenges and opportunities. *Trends Pharmacol. Sci.* **33,** 394–404

15. Fitzgerald, M. L., Mujawar, Z., and Tamehiro, N. (2010) ABC transporters, atherosclerosis and inflammation. *Atherosclerosis* **211,** 361–370

16. Ito, A., Hong, C., Rong, X., Zhu, X., Tarling, E. J., Hedde, P. N., Gratton, E., Parks, J., and Tontonoz, P. (2015) LXRs link metabolism to inflammation through Abca1-dependent regulation of membrane composition and TLR signaling. *Elife* **4,** e08009

17. Bochem, A. E., van der Valk, F. M., Tolani, S., Stroes, E. S., Westerterp, M., and Tall, A. R. (2015) Increased systemic and plaque inflammation in ABCA1 mutation carriers with attenuation by statins. *Arterioscler. Thromb. Vasc. Biol.* **35,** 1663–1669

18. Tang, C., Houston, B. A., Storey, C., and LeBoeuf, R. C. (2016) Both STAT3 activation and cholesterol efflux contribute to the anti-inflammatory effect of apoA-I/ABCA1 interaction in macrophages. *J. Lipid Res.* **57,** 848–857

19. Wu, C. H., Chen, C. C., Lai, C. Y., Hung, T. H., Lin, C. C., Chao, M., and Chen, S. F. (2016) Treatment with TO901317, a synthetic liver X receptor agonist, reduces brain damage and attenuates neuroinflammation in experimental intracerebral hemorrhage. *J. Neuroinflammation* **13,** 62

20. Björkhem, I. (2009) Are side-chain oxidized oxysterols regulators also *in vivo*? *J. Lipid Res.* **50,** S213–S218

21. Björkhem, I. (2013) Five decades with oxysterols. *Biochimie* **95,** 448–454

22. Björkhem, I. (2002) Do oxysterols control cholesterol homeostasis? *J. Clin. Invest.* **110,** 725–730

23. Janowski, B. A., Grogan, M. J., Jones, S. A., Wisely, G. B., Kliewer, S. A., Corey, E. J., and Mangelsdorf, D. J. (1999) Structural requirements of ligands for the oxysterol liver X receptors LXRα and LXRβ. *Proc. Natl. Acad. Sci. U.S.A.* **96,** 266–271

24. Nieva, J., Shafton, A., Altobell, L. J., 3rd, Tripuraneni, S., Rogel, J. K., Wentworth, A. D., Lerner, R. A., and Wentworth, P., Jr. (2008) Lipid-derived aldehydes accelerate light chain amyloid and amorphous aggregation. *Biochemistry* **47,** 7695–7705

25. Stewart, C. R., Wilson, L. M., Zhang, Q., Pham, C. L., Waddington, L. J., Staples, M. K., Stapleton, D., Kelly, J. W., and Howlett, G. J. (2007) Oxidized cholesterol metabolites found in human atherosclerotic lesions promote apolipoprotein C-II amyloid fibril formation. *Biochemistry* **46,** 5552–5561

26. Wentworth, A. D., Song, B. D., Nieva, J., Shafton, A., Tripurenani, S., and Wentworth, P., Jr. (2009) The ratio of cholesterol 5,6-secosterols formed from ozone and singlet oxygen offers insight into the oxidation of cholesterol in vivo. *Chem. Commun.* 2009, 3098–4100

27. Pulfer, M. K., and Murphy, R. C. (2004) Formation of biologically active oxysterols during ozonolysis of cholesterol present in lung surfactant. *J. Biol. Chem.* **279,** 26331–26338

28. Almstrand, A. C., Voelker, D., and Murphy, R. C. (2015) Identification of oxidized phospholipids in bronchoalveolar lavage exposed to low ozone levels using multivariate analysis. *Anal. Biochem.* **474,** 50–58

29. Windsor, K., Genaro-Mattos, T. C., Miyamoto, S., Stec, D. F., Kim, H. Y., Tallman, K. A., and Porter, N. A. (2014) Assay of protein and peptide adducts of cholesterol ozonolysis products by hydrophobic and click enrichment methods. *Chem. Res. Toxicol.* **27,** 1757–1768

30. Bauer, R. N., Müller, L., Brighton, L. E., Duncan, K. E., and Jaspers, I. (2015) Interaction with epithelial cells modifies airway macrophage response to ozone. *Am. J. Respir. Cell Mol. Biol.* **52,** 285–294

31. Jaspers, I., Flescher, E., and Chen, L. C. (1997) Ozone-induced IL-8 expression and transcription factor binding in respiratory epithelial cells. *Am. J. Physiol.* **272,** L504–L511

32. Windsor, K., Genaro-Mattos, T. C., Kim, H. Y., Liu, W., Tallman, K. A., Miyamoto, S., Korade, Z., and Porter, N. A. (2013) Probing lipid-protein adduction with alkynyl surrogates: application to Smith-Lemli-Opitz syndrome. *J. Lipid Res.* **54,** 2842–2850

33. Connor, R. E., Marnett, L. J., and Liebler, D. C. (2011) Protein-selective capture to analyze electrophile adduction of Hsp90 by 4-hydroxynonenal. *Chem. Res. Toxicol.* **24,** 1275–1282

34. Hemming, J. M., Hughes, B. R., Rennie, A. R., Tomas, S., Campbell, R. A., Hughes, A. V., Arnold, T., Botchway, S. W., and Thompson, K. C. (2015) Environmental pollutant ozone causes damage to lung surfactant protein B (SP-B). *Biochemistry* **54,** 5185–5197

35. Uhlson, C., Harrison, K., Allen, C. B., Ahmad, S., White, C. W., and Murphy, R. C. (2002) Oxidized phospholipids derived from ozone-treated lung surfactant extract reduce macrophage and epithelial cell viability. *Chem. Res. Toxicol.* **15,** 896–906

36. Oosting, R. S., van Greevenbroek, M. M., Verhoef, J., van Golde, L. M., and Haagsman, H. P. (1991) Structural and functional changes of surfactant protein A induced by ozone. *Am. J. Physiol.* **261,** L77–L83

37. Sayre, L. M., Lin, D., Yuan, Q., Zhu, X., and Tang, X. (2006) Protein adducts generated from products of lipid oxidation: focus on HNE and one. *Drug Metab. Rev.* **38,** 651–675

38. Uchida, K., Shiraishi, M., Naito, Y., Torii, Y., Nakamura, Y., and Osawa, T. (1999) Activation of stress signaling pathways by the end product of lipid peroxidation. 4-Hydroxy-2-nonenal is a potential inducer of intracellular peroxide production. *J. Biol. Chem.* **274,** 2234–2242

39. Kim, H. Y., Tallman, K. A., Liebler, D. C., and Porter, N. A. (2009) An azido-biotin reagent for use in the isolation of protein adducts of lipid-derived electrophiles by streptavidin catch and photorelease. *Mol. Cell. Proteomics* **8,** 2080–2089

40. Forman, B. M., Tontonoz, P., Chen, J., Brun, R. P., Spiegelman, B. M., and Evans, R. M. (1995) 15-Deoxy-Δ12,14-prostaglandin J2 is a ligand for the adipocyte determination factor PPARγ. *Cell* **83,** 803–812

41. Ulven, S. M., Dalen, K. T., Gustafsson, J. A., and Nebb, H. I. (2005) LXR is crucial in lipid metabolism. *Prostaglandins Leukot. Essent. Fatty Acids* **73,** 59–63

42. Joseph, S. B., Bradley, M. N., Castrillo, A., Bruhn, K. W., Mak, P. A., Pei, L., Hogenesch, J., O'connell, R. M., Cheng, G., Saez, E., Miller, J. F., and Tontonoz, P. (2004) LXR-dependent gene expression is important for macrophage survival and the innate immune response. *Cell* **119,** 299–309

43. Gowdy, K. M., and Fessler, M. B. (2013) Emerging roles for cholesterol and lipoproteins in lung disease. *Pulm. Pharmacol. Ther.* **26,** 430–437

44. Azzam, K. M., and Fessler, M. B. (2012) Crosstalk between reverse cholesterol transport and innate immunity. *Trends Endocrinol. Metab.* **23,** 169–178

45. Draper, D. W., Gowdy, K. M., Madenspacher, J. H., Wilson, R. H., Whitehead, G. S., Nakano, H., Pandiri, A. R., Foley, J. F., Remaley, A. T., Cook, D. N., and Fessler, M. B. (2012) ATP binding cassette transporter G1 deletion induces IL-17-dependent dysregulation of pulmonary adaptive immunity. *J. Immunol.* **188,** 5327–5336

46. Smoak, K., Madenspacher, J., Jeyaseelan, S., Williams, B., Dixon, D., Poch, K. R., Nick, J. A., Worthen, G. S., and Fessler, M. B. (2008) Effects of liver X receptor agonist treatment on pulmonary inflammation and host defense. *J. Immunol.* **180,** 3305–3312

47. Gong, H., He, J., Lee, J. H., Mallick, E., Gao, X., Li, S., Homanics, G. E., and Xie, W. (2009) Activation of the liver X receptor prevents lipopolysaccharide-induced lung injury. *J. Biol. Chem.* **284,** 30113–30121

48. Crisafulli, C., Mazzon, E., Paterniti, I., Galuppo, M., Bramanti, P., and Cuzzocrea, S. (2010) Effects of liver X receptor agonist treatment on signal transduction pathways in acute lung inflammation. *Respir. Res.* **11,** 19

49. Fu, X., Menke, J. G., Chen, Y., Zhou, G., MacNaul, K. L., Wright, S. D., Sparrow, C. P., and Lund, E. G. (2001) 27-Hydroxycholesterol is an endogenous ligand for liver X receptor in cholesterol-loaded cells. *J. Biol. Chem.* **276,** 38378–38387

50. Alexis, N. E., Lay, J. C., Hazucha, M., Harris, B., Hernandez, M. L., Bromberg, P. A., Kehrl, H., Diaz-Sanchez, D., Kim, C., Devlin, R. B., and Peden, D. B. (2010) Low-level ozone exposure induces airways inflammation and modifies cell surface phenotypes in healthy humans. *Inhal. Toxicol.* **22,** 593–600

51. Jörres, R. A., Holz, O., Zachgo, W., Timm, P., Koschyk, S., Müller, B., Grimminger, F., Seeger, W., Kelly, F. J., Dunster, C., Frischer, T., Lubec, G., Waschewski, M., Niendorf, A., and Magnussen, H. (2000) The effect of repeated ozone exposures on inflammatory markers in bronchoalveolar lavage fluid and mucosal biopsies. *Am. J. Respir. Crit. Care Med.* **161,** 1855–1861

52. Wang, D., Liu, M., Wang, Y., Luo, M., Wang, J., Dai, C., Yan, P., Zhang, X., Wang, Y., Tang, C., and Xiao, J. (2011) Synthetic LXR agonist T0901317 attenuates lipopolysaccharide-induced acute lung injury in rats. *Int. Immunopharmacol.* **11,** 2098–2103

53. Kim, H. J., Yoon, K. A., Yoon, H. J., Hong, J. M., Lee, M. J., Lee, I. K., and Kim, S. Y. (2013) Liver X receptor activation inhibits osteoclastogenesis by suppressing NF-κB activity and c-Fos induction and prevents inflammatory bone loss in mice. *J. Leukocyte Biol.* **94,** 99–107

54. Zelcer, N., and Tontonoz, P. (2006) Liver X receptors as integrators of metabolic and inflammatory signaling. *J. Clin. Invest.* **116,** 607–614

55. Solan, P. D., Piraino, G., Hake, P. W., Denenberg, A., O'Connor, M., Lentsch, A., and Zingarelli, B. (2011) Liver X receptor α activation with the synthetic ligand T0901317 reduces lung injury and inflammation after hemorrhage and resuscitation via inhibition of the nuclear factor κB pathway. *Shock* **35,** 367–374

56. Joseph, S. B., Castrillo, A., Laffitte, B. A., Mangelsdorf, D. J., and Tontonoz, P. (2003) Reciprocal regulation of inflammation and lipid metabolism by liver X receptors. *Nat. Med.* **9,** 213–219

57. Ghisletti, S., Huang, W., Jepsen, K., Benner, C., Hardiman, G., Rosenfeld, M. G., and Glass, C. K. (2009) Cooperative NCoR/SMRT interactions establish a corepressor-based strategy for integration of inflammatory and anti-inflammatory signaling pathways. *Genes Dev.* **23,** 681–693

58. Venteclef, N., Jakobsson, T., Ehrlund, A., Damdimopoulos, A., Mikkonen, L., Ellis, E., Nilsson, L. M., Parini, P., Jänne, O. A., Gustafsson, J. A., Steffensen, K. R., and Treuter, E. (2010) GPS2-dependent corepressor/SUMO pathways govern anti-inflammatory actions of LRH-1 and LXRβ in the hepatic acute phase response. *Genes Dev.* **24,** 381–395

59. Treuter, E., and Venteclef, N. (2011) Transcriptional control of metabolic and inflammatory pathways by nuclear receptor SUMOylation. *Biochim. Biophys. Acta* **1812,** 909–918

60. Ghisletti, S., Huang, W., Ogawa, S., Pascual, G., Lin, M. E., Willson, T. M., Rosenfeld, M. G., and Glass, C. K. (2007) Parallel SUMOylation-dependent pathways mediate gene- and signal-specific transrepression by LXRs and PPARγ. *Mol. Cell* **25,** 57–70

61. Miyata, R., Bai, N., Vincent, R., Sin, D. D., and Van Eeden, S. F. (2013) Statins reduce ambient particulate matter-induced lung inflammation by promoting the clearance of particulate matter, <10 μm from lung tissues. *Chest* **143,** 452–460

62. Ostro, B., Malig, B., Broadwin, R., Basu, R., Gold, E. B., Bromberger, J. T., Derby, C., Feinstein, S., Greendale, G. A., Jackson, E. A., Kravitz, H. M., Matthews, K. A., Sternfeld, B., Tomey, K., Green, R. R., and Green, R. (2014) Chronic PM2.5 exposure and inflammation: determining sensitive subgroups in mid-life women. *Environ. Res.* **132,** 168–175

63. O'Neill, M. S., Veves, A., Sarnat, J. A., Zanobetti, A., Gold, D. R., Economides, P. A., Horton, E. S., and Schwartz, J. (2007) Air pollution and inflammation in type 2 diabetes: a mechanism for susceptibility. *Occup. Environ. Med.* **64,** 373–379

64. Zanobetti, A., Schwartz, J., and Ridker, P. M. (2004) Air pollution and markers of cardiovascular risk. *Epidemiology* **15,** S22

65. Fessler, M. B. (2009) Simvastatin as a potential therapeutic for acute respiratory distress syndrome. *Am. J. Respir. Crit. Care Med.* **180,** 1031

66. Devlin, R. B., McDonnell, W. F., Becker, S., Madden, M. C., McGee, M. P., Perez, R., Hatch, G., House, D. E., and Koren, H. S. (1996) Time-dependent changes of inflammatory mediators in the lungs of humans exposed to 0.4 ppm ozone for 2 hr: a comparison of mediators found in bronchoalveolar lavage fluid 1 and 18 hr after exposure. *Toxicol. Appl. Pharmacol.* **138,** 176–185

67. Lopez-Souza, N., Avila, P. C., and Widdicombe, J. H. (2003) Polarized cultures of human airway epithelium from nasal scrapings and bronchial brushings. *In Vitro Cell. Dev. Biol. Anim.* **39,** 266–269

68. Müller, L., Brighton, L. E., and Jaspers, I. (2013) Ozone exposed epithelial cells modify cocultured natural killer cells. *Am. J. Physiol. Lung Cell. Mol. Physiol.* **304,** L332–L341

69. Kesic, M. J., Meyer, M., Bauer, R., and Jaspers, I. (2012) Exposure to ozone modulates human airway protease/antiprotease balance contributing to increased influenza A infection. *PLoS ONE* **7,** e35108

Oxysterol and Lipid-Protein Adducts

70. Kim, C. S., Alexis, N. E., Rappold, A. G., Kehrl, H., Hazucha, M. J., Lay, J. C., Schmitt, M. T., Case, M., Devlin, R. B., Peden, D. B., and Diaz-Sanchez, D. (2011) Lung function and inflammatory responses in healthy young adults exposed to 0.06 ppm ozone for 6.6 hours. *Am. J. Respir. Crit. Care Med.* **183,** 1215–1221

71. Jaspers, I., Zhang, W., Fraser, A., Samet, J. M., and Reed, W. (2001) Hydrogen peroxide has opposing effects on IKK activity and IκBα breakdown in airway epithelial cells. *Am. J. Respir. Cell Mol. Biol.* **24,** 769–777

72. Jaspers, I., Ciencewicki, J. M., Zhang, W., Brighton, L. E., Carson, J. L., Beck, M. A., and Madden, M. C. (2005) Diesel exhaust enhances influenza virus infections in respiratory epithelial cells. *Toxicol. Sci.* **85,** 990–1002

73. Liu, W., Xu, L., Lamberson, C. R., Merkens, L. S., Steiner, R. D., Elias, E. R., Haas, D., and Porter, N. A. (2013) Assays of plasma dehydrocholesteryl esters and oxysterols from Smith-Lemli-Opitz syndrome patients. *J. Lipid Res.* **54,** 244–253

74. Madenspacher, J. H., Azzam, K. M., Gowdy, K. M., Malcolm, K. C., Nick, J. A., Dixon, D., Aloor, J. J., Draper, D. W., Guardiola, J. J., Shatz, M., Menendez, D., Lowe, J., Lu, J., Bushel, P., Li, L., Merrick, B. A., *et al.* (2013) p53 Integrates host defense and cell fate during bacterial pneumonia. *J. Exp. Med.* **210,** 891–904

75. Hong, V., Presolski, S. I., Ma, C., and Finn, M. G. (2009) Analysis and optimization of copper-catalyzed azide-alkyne cycloaddition for bioconjugation. *Angew. Chem. Int. Ed. Engl.* **48,** 9879–9883

76. Tal, T. L., Simmons, S. O., Silbajoris, R., Dailey, L., Cho, S. H., Ramabhadran, R., Linak, W., Reed, W., Bromberg, P. A., and Samet, J. M. (2010) Differential transcriptional regulation of IL-8 expression by human airway epithelial cells exposed to diesel exhaust particles. *Toxicol. Appl. Pharmacol.* **243,** 46–54